Springer

Dear Author,

Here are the proofs of your article.

- You can submit your corrections **online** or by **fax**.
- For **online** submission please insert your corrections in the online correction form. Always indicate the line number to which the correction refers.
- Please return your proof together with the **permission to publish** confirmation.
- For **fax** submission, please ensure that your corrections are clearly legible. Use a fine black pen and write the correction in the margin, not too close to the edge of the page.
- Remember to note the journal title, article number, and your name when sending your response via e-mail, fax or regular mail.
- **Check** the metadata sheet to make sure that the header information, especially author names and the corresponding affiliations are correctly shown.
- **Check** the questions that may have arisen during copy editing and insert your answers/ corrections.
- **Check** that the text is complete and that all figures, tables and their legends are included. Also check the accuracy of special characters, equations, and electronic supplementary material if applicable. If necessary refer to the *Edited manuscript*.
- The publication of inaccurate data such as dosages and units can have serious consequences. Please take particular care that all such details are correct.
- Please **do not** make changes that involve only matters of style. We have generally introduced forms that follow the journal's style.
  Substantial changes in content, e.g., new results, corrected values, title and authorship are not allowed without the approval of the responsible editor. In such a case, please contact the Editorial Office and return his/her consent together with the proof.
- If we do not receive your corrections **within 48 hours**, we will send you a reminder.

Please note

Your article will be published **Online First** approximately one week after receipt of your corrected proofs. This is the **official first publication** citable with the DOI. **Further changes are, therefore, not possible**.

After online publication, subscribers (personal/institutional) to this journal will have access to the complete article via the DOI using the URL: http://dx.doi.org/[DOI].

If you would like to know when your article has been published online, take advantage of our free alert service. For registration and further information go to: www.springerlink.com.

Due to the electronic nature of the procedure, the manuscript and the original figures will only be returned to you on special request. When you return your corrections, please inform us, if you would like to have these documents returned.

The **printed version** will follow in a forthcoming issue.

Fax to: +1 347 649 2158 (US) or +44 207 806 8278 (UK) or +91 44 4208 9499 (INDIA)

To: **Springer Correction Team**
6&7, 5th Street, Radhakrishnan Salai, Chennai, Tamil Nadu, India – 600004
e-mail: spr_corrections2@sps.co.in

Re: Cell Biochemistry and Biophysics DOI:10.1007/s12013-008-9034-3
Exchange of Microtubule Molecular Motors During Melanosome Transport in Xenopus laevis Melanophores is Triggered by Collisions with Intracellular Obstacles

Authors: Luciana Bruno · Mercedes Echarte · Valeria Levi

Permission to publish

I have checked the proofs of my article and

- ❑ I have no corrections. The article is ready to be published without changes.
- ❑ I have a few corrections. I am enclosing the following pages:
- ❑ I have made many corrections. Enclosed is the complete article.

Date / signature _____

Metadata of the article that will be visualized in OnlineFirst

Please note: Images will appear in color online but will be printed in black and white.

ArticleTitle	Exchange of Microtubule Molecular Motors During Melanosome Transport in *Xenopus laevis* Melanophores is Triggered by Collisions with Intracellular Obstacles	
Article Sub-Title		
Article CopyRight - Year	Humana Press Inc. 2008 (This will be the copyright line in the final PDF)	
Journal Name	Cell Biochemistry and Biophysics	
Corresponding Author	Family Name	**Levi**
	Particle	
	Given Name	**Valeria**
	Suffix	
	Division	Departamento de Física, Facultad de Ciencias Exactas y Naturales
	Organization	Universidad de Buenos Aires
	Address	Pabellón 1, Ciudad Universitaria, CP 1428, Ciudad de Buenos Aires, Argentina
	Email	vlevi@df.uba.ar
Author	Family Name	**Bruno**
	Particle	
	Given Name	**Luciana**
	Suffix	
	Division	Departamento de Física, Facultad de Ciencias Exactas y Naturales
	Organization	Universidad de Buenos Aires
	Address	Pabellón 1, Ciudad Universitaria, CP 1428, Ciudad de Buenos Aires, Argentina
	Email	
Author	Family Name	**Echarte**
	Particle	
	Given Name	**Mercedes**
	Suffix	
	Division	
	Organization	Unidad Integrada INTA Balcarce, Facultad de Ciencias Agrarias
	Address	Ruta Nacional 226 km 73.5, CC 226, 7620, Balcarce, Argentina
	Email	

Schedule	Received	
	Revised	
	Accepted	

Abstract The observation that several cargoes move bidirectionally along microtubules in vivo raised the question regarding how molecular motors with opposed polarity coordinate during transport. In this work, we analyzed the switch of microtubule motors during the transport of melanosomes in *Xenopus* melanophores by registering trajectories of these organelles moving along microtubules using a fast and precise tracking method. We analyzed in detail the intervals of trajectories showing reversions in the original direction of transport and processive motion in the opposite direction for at least 250 nm. In most of the cases, the speed of the melanosome before the reversion slowly decreases with time approaching zero then, the organelle returns over the same path moving initially at a very high speed and slowing down with time. These results

could be explained according to a model in which reversions are triggered by an elastic collision of the cargo with obstacles in the cytosol. This interaction generates a force opposed to the movement of the motor-driven organelle increasing the probability of detaching the active motors from the track. The model can explain reversions in melanosome trajectories as well as other characteristics of in vivo transport along microtubules observed by other authors. Our results suggest that the crowded cytoplasm plays a key role in regulating the coordination of microtubules-dependent motors.

Keywords (separated by '-')	Microtubule molecular motors - *Xenopus* melanophores - Coordination - Melanosome transport
Footnote Information	**Electronic supplementary material** The online version of this article (doi:10.1007/s12013-008-9034-3) contains supplementary material, which is available to authorized users.

Metadata of the article that will be visualized in OnlineAlone

Electronic supplementary material	(AVI 15302 kb)

Journal:	12013
Article:	9034

Author Query Form

Springer
the language of science

Please ensure you fill out your response to the queries raised below and return this form along with your corrections

Dear Author,

During the preparation of your manuscript for typesetting, some questions have arisen. These are listed below. Please check your typeset proof carefully and mark any corrections in the margin of the proof or compile them as a separate list. This form should then be returned with your marked proof/list of corrections to spr_corrections2@sps.co.in

Disk use

In some instances we may be unable to process the electronic file of your article and/or artwork. In that case we have, for efficiency reasons, proceeded by using the hard copy of your manuscript. If this is the case the reasons are indicated below:

❑ Disk damaged ❑ Incompatible file format ❑ LaTeX file for non-LaTeX journal
❑ Virus infected ❑ Discrepancies between electronic file and (peer-reviewed, therefore definitive) hard copy
❑ Other: .....

We have proceeded as follows:

❑ Manuscript scanned ❑ Manuscript keyed in ❑ Artwork scanned
❑ Files only partly used (parts processed differently: ……...……..)

Bibliography

If discrepancies were noted between the literature list and the text references, the following may apply:

❑ The references listed below were noted in the text but appear to be missing from your literature list. Please complete the list or remove the references from the text.
❑ *Uncited references*: This section comprises references that occur in the reference list but not in the body of the text. Please position each reference in the text or delete it. Any reference not dealt with will be retained in this section.

Queries and/or remarks

Section/paragraph	Details required	Author's response
A Model for Wave-Shaped Reversions/Para 8	The equation next to equation (2) is been numbered as equation (5). Hence, we have renumbered it as equation (3). Please confirm.	

Cell Biochem Biophys
DOI 10.1007/s12013-008-9034-3

ORIGINAL PAPER

Exchange of Microtubule Molecular Motors During Melanosome Transport in *Xenopus laevis* Melanophores is Triggered by Collisions with Intracellular Obstacles

Luciana Bruno · Mercedes Echarte · Valeria Levi

Abstract The observation that several cargoes move bidirectionally along microtubules in vivo raised the question regarding how molecular motors with opposed polarity coordinate during transport. In this work, we analyzed the switch of microtubule motors during the transport of melanosomes in *Xenopus* melanophores by registering trajectories of these organelles moving along microtubules using a fast and precise tracking method. We analyzed in detail the intervals of trajectories showing reversions in the original direction of transport and processive motion in the opposite direction for at least 250 nm. In most of the cases, the speed of the melanosome before the reversion slowly decreases with time approaching zero then, the organelle returns over the same path moving initially at a very high speed and slowing down with time. These results could be explained according to a model in which reversions are triggered by an elastic collision of the cargo with obstacles in the cytosol. This interaction generates a force opposed to the movement of the motor-driven organelle increasing the probability of detaching the active motors from the track. The model can explain reversions in melanosome trajectories as well as other characteristics of in vivo transport along microtubules observed by other authors. Our results suggest that the crowded cytoplasm plays a key role in regulating the coordination of microtubules-dependent motors.

Keywords Microtubule molecular motors · *Xenopus* melanophores · Coordination · Melanosome transport

Introduction

Molecular motors are responsible for the transport of a wide variety of components, which are positioned in the cytoplasm in a precise spatio-temporal manner. There are three families of motors involved in the transport of cargoes in the cell cytoplasm: myosin motors which move along actin filaments; as well as kinesin and dynein motors that move along microtubules toward their plus- and minus-end, respectively (reviewed in [1]).

The involvement of two motors of opposite polarity in organelle transport along microtubules raised the question about how transport is regulated along these cytoskeleton tracks. In several cellular systems it was observed that cargoes initially transported toward the microtubule minus-end frequently changed their direction and moved toward the plus-end and vice versa (see for example, [2–8]).

Three different models have been proposed to explain these experimental observations (reviewed in [1, 9, 10]).

According to the first model, opposed-polarity motors are involved in a tug-of-war with the stronger motor determining the direction of motion at any particular moment. This model predicts, for example, that the impairment of the plus-end directed transport should improve the instantaneous transport in the opposite direction. However, it has been shown that mutations which damage the functionality of kinesin-II during pigment

Electronic supplementary material The online version of this article (doi:10.1007/s12013-008-9034-3) contains supplementary material, which is available to authorized users.

L. Bruno · V. Levi (✉)
Departamento de Física, Facultad de Ciencias Exactas y Naturales, Universidad de Buenos Aires, Pabellón 1, Ciudad Universitaria, CP 1428 Ciudad de Buenos Aires, Argentina
e-mail: vlevi@df.uba.ar

M. Echarte
Unidad Integrada INTA Balcarce, Facultad de Ciencias Agrarias, Ruta Nacional 226 km 73.5, CC 226, 7620 Balcarce, Argentina

Humana Press

Journal : Large 12013 | Dispatch : 28-10-2008 | Pages : 11
Article No. : 9034 | ☐ LE | ☐ TYPESET
MS Code : EM522 | ☑ CP | ☑ DISK

organelle transport in melanophores cells or of dynein or the dynactin complex in the case of lipid droplets transport in *Drosophila* embryos do not improve the transport in the opposite direction [10, 11].

The exclusionary presence model considers that while both types of motors can bind to a cargo, they cannot both do it at the same time. However, the total amount of either plus- or minus-end directed motors that is attached to a pigment organelle in frog melanophores does not change when stimulating the transport toward the plus- or the minus-end of the microtubules [11] in opposition to what it would be expected according to this model.

These and other experimental finding from several cellular systems support the coordination model to explain regulation of transport along microtubules (reviewed in [9]). According to this model, kinesin and dynein are simultaneously present on cellular cargo and their activities are coordinated so that when plus-end motors are active, minus-end motors are not, and vice versa.

The precise mechanism of coordination is still unknown; however, some protein complexes have been proposed to mediate the coordination between motors [12–14]. Dynactin is a potential candidate for coordination of microtubule-dependent motors in frog melanocytes [15]. Minus- and plus-end motors compete for binding to the same region of this protein complex and impairment of dynactin abolishes both plus- and minus-end motion of several bidirectional cargoes [8, 15]. Moreover, dynactin increases the processivity of kinesin-2 [16] and of cytoplasmic dynein, which is not processive in the absence of this protein complex [17].

Regardless of the exact nature of how coordination is achieved, the process that triggers the switch of motors remains unexplained. In this article, we address this issue by studying reversions in trajectories of organelles transported by microtubule-dependent motors in *Xenopus laevis* melanophores.

Melanophores cells are one of the cellular systems commonly used to study the function of molecular motors in vivo (reviewed in [18]). The major physiological task of these cells is to move pigment organelles called melanosomes in the cytoplasm, allowing animals to display color change. *Xenopus* melanophores have melanosomes filled with the black pigment melanin, and therefore these organelles can be easily imaged and discriminated from other cellular components using brightfield transmission microscopy without the need of any contrast generation technique or the use of fluorescent probes.

The transport of melanosomes is regulated by signaling cascades initiated by the binding of specific hormones to cell-surface receptors, which results in the modulation of cAMP concentrations in the cytoplasm [19, 20]. Therefore, one can stimulate melanosome movement toward or away from the cell center by using appropriate hormones to decrease or increase the concentration of cAMP, respectively. While melatonin increases the amount of cAMP triggering aggregation of melanosomes towards the perinuclear region, MSH (melanocyte stimulating hormone) reduces cAMP concentration and thus promotes melanosomes dispersion in the cytoplasm [18]. Importantly, the observation of bidirectional motion of melanosomes during aggregation and dispersion indicates that kinesin and dynein motors alternates in the transport of these cargoes. To achieve the characteristic distributions of melanosomes observed during aggregation and dispersion, minus-end directed motion dominates during aggregation while plus-end directed motion dominates during dispersion [9].

Melanosome transport in *Xenopus* melanophores is well characterized in terms of molecular motors participating in the movement. Transport along microtubules is driven by kinesin-2 [21] and cytoplasmic dynein [22], and myosin-V transports melanosomes along actin filaments [23]. It is possible to eliminate the contribution of myosin-V to melanosome movement by depolymerizing actin filaments with latrunculin B. The remaining movement is entirely microtubule dependent and therefore, latrunculin-treated cells can be used to study the contribution of microtubule motors cytoplasmic dynein and kinesin-2 to organelle transport without the contribution of the second transport system [11].

In this work, we analyzed the switch of microtubule motors during transport of melanosomes in *Xenopus* melanophores by registering trajectories of these organelles moving along microtubules using a fast and precise tracking method. We analyzed in detail the intervals of trajectories showing reversions in the original direction of transport that can be associated with a switch between the microtubule-dependent motors responsible for the transport. The experimental data could be explained considering that reversions are triggered by an elastic collision of the cargo with obstacles in the cytosol. Our results suggest that the crowded cytoplasm plays a key role in regulating the switching of microtubules-dependent motors.

Materials and Methods

Cell Culture and Samples Preparation for Imaging

Immortalized *Xenopus laevis* melanophores were cultured as described [24]. In order to track the movement of individual organelles, the number of melanosomes in the cell was reduced by treatment with phenylthiourea [11].

For microscopy measurements, cells were grown for 2 days on 25-mm round polylysine-coated coverslips placed into 35-mm plates in 2.5 ml of the medium. Before observation, the coverslips were washed in serum-free 70%

Journal : Large 12013 | Dispatch : 28-10-2008 | Pages : 11
Article No. : 9034 | LE | TYPESET
MS Code : EM522 | CP | DISK

L-15 medium and mounted in a custom-made chamber specially designed for the microscope. The cells were treated with 10 μM latrunculin B (Biomol International, Plymouth Meeting, PA) for at least 30 min to depolymerize actin filaments. Melanophores were stimulated for aggregation or dispersion with 10 nM melatonin or 100 nM MSH, respectively. Samples were observed between 5 and 15 min after stimulation. All measurements were performed at 21°C.

Microscope Setup

Tracking experiments were carried out in an Olympus IX70 microscope using a 60× water-immersion objective (numerical aperture = 1.2) under illumination with a tungsten-halogen lamp. A cMOS camera (Pixelink, Ottawa, Ontario, Canada) was attached to the video port of the microscope for imaging the cells. Movies were registered at a speed of 100 frame/s. The pixel size was 120 nm and was set following the criteria discussed in Thompson et al. [25].

Experiments are controlled by the acquisition program Globals for Images, program developed at the Laboratory for Fluorescence Dynamics (UCI, Irvine, CA).

Pattern-Recognition Algorithm for Tracking Melanosomes

The pattern-recognition tracking routine is described in [26]. Briefly, the program starts the tracking routine displaying the first frame of the image stack under analysis. The operator chooses the target melanosome by simply clicking on top of its image. Doing so, the program sets the initial coordinates of the melanosome and generates an intensity pattern that consists of the average intensity obtained from the first 10 frames of a region containing the melanosome image. This pattern is stored in the computer memory to be used during the calculation of the melanosome position through the image stack. In the following frames, the pattern is shifted around the position determined for the particle in the previous frame and a parameter σ that scores the absolute intensity differences between image and pattern is calculated. The σ value will be minimal when the image in the frame matches the pattern features, thus it can identify the particle of interest from other structures present in the frame [27]. Another advantage is that the method does not need a theoretical expression for the intensity distribution of the particle as Gaussian fitting methods [28]. The particle position is calculated with sub-pixel resolution by determining the position corresponding to the minimum value of σ with a parabolic interpolation. By using this method, we could recover the position of 500 nm particles with 2 nm precision and 10 ms temporal resolution [26].

Reversion-Finder Method

We define long-term reversions as those segments of the trajectories in which the melanosome travels back over the same path for at least 250 nm (i.e., the average radius of a melanosome [24]) during more than 1 s. Importantly, this distance is much longer than the level of noise commonly observed in the trajectories ($\sim$10 nm). This criterion allows excluding spontaneous, short-term reversions due to, e.g., thermal jittering or external noise from the analysis.

To automatically detect reversions in trajectories we scored each pair of a trajectory data points with a parameter D_{ij} defined as $D_{ij} = l_{ij}/d_{ij}$, where d_{ij} is the point-to-point Euclidean distance and l_{ij} is the distance along the trajectory between the same pair of data points.

Points belonging to a reversion will have high D_{ij} values. We constructed an algorithm that select regions with D_{ij} values higher than a threshold set to 10. These regions were considered part of reversions if they also fulfill the requirements presented above. To speed up the computational time without loosing critical information, only 1 of 10 contiguous data points were considered in this initial analysis.

The procedure described above was implemented using Matlab (The MathWorks, Natick, MA) routines.

Results and Discussion

Reversions in Trajectories of Melanosomes During Aggregation and Dispersion

Melanophores were incubated with latrunculin B as indicated in Materials and Methods in order to depolymerize the actin filaments. Aggregation or dispersion of melanosomes was induced by addition of melatonin and MSH, respectively. We recorded 10–20 movies per cell after incubating them for at least 5 min and no more than 15 min in the presence of either melatonin or MSH.

To have a precise description of melanosome motion we used a fast tracking routine that allow us to recover the melanosome position with 2 nm precision and 10 ms temporal resolution. One of the advantages of the method is that it does not assume any intensity distribution for the particle image and thus it can be used to track, for example, micrometer-sized particles such as melanosomes. We have previously used this method to study melanosome transport along microtubules [26] and actin filaments [29].

Three hundred total trajectories of melanosomes moving after stimulating cells for aggregation or dispersion were determined from the movies using the pattern-recognition algorithm described above and were classified according to the direction in which the melanosome was initially

Journal : Large 12013 Dispatch : 28-10-2008 Pages : 11
Article No. : 9034 LE TYPESET
MS Code : EM522 CP DISK

moving. Microtubules minus-ends are attached to the centrosome, which is located near the nucleus. Therefore, those trajectories showing a preferential direction toward the perinuclear region correspond mainly to organelles transported by cytoplasmic dynein while those moving toward the cell periphery are generally transported by kinesin 2. In this article, we assigned inward and outward motion of melanosomes to transport driven by dynein and kinesin, respectively. It is important to mention that while most of inward and outward trajectories will in fact correspond to the assigned motors, we cannot be sure about the identity of the motor in every analyzed trajectory.

Figure 1 shows an example of a trajectory obtained for a melanosome moving after stimulating the cells with melatonin. In this particular trajectory, the organelle moves toward the cell nucleus probably by the action of cytoplasmic dynein and it suddenly reverts its direction being transported backwards by kinesin-2 toward the cell periphery. A similar behavior can also be observed in the supplemental movie 1, which shows a representative tracking experiment.

To quantify the probability of reversion during in vivo transport, we constructed a reversion-finder algorithm that allow us to detect those regions of the trajectories in which organelles originally moving in a given direction show afterwards a continuous sustainable motion in the opposite direction for more than 250 nm during at least 1 s (see Materials and Methods). These arbitrary thresholds were set to exclude from the analysis dubious reversions that could be consequence of other processes.

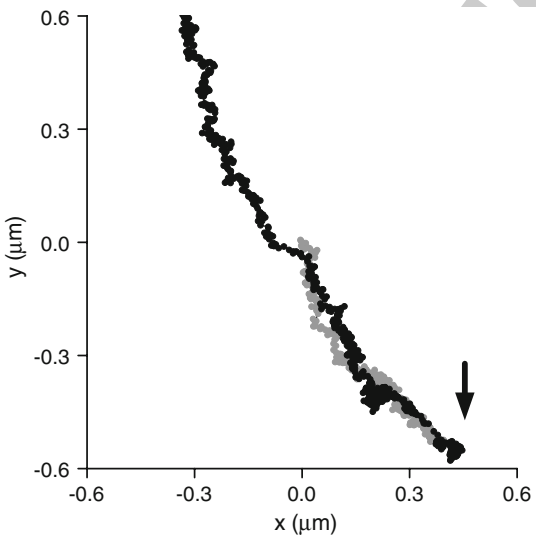

Fig. 1 Reversals in melanosome trajectories. Example of a trajectory obtained for a melanosome that was initially transported by cytoplasmic dynein (gray) and suddenly reverts its direction moving finally toward the cell periphery by the action of kinesin-2 (black). The switch point is marked with an arrow. The trajectory lasted 9.8 s

In total, 30 and 40% of the trajectories determined for melanosomes during dispersion and aggregation, respectively, presented long-range reversions indicating that they are frequent processes during organelle transport (Table 1).

We determined the relative reversion probability of organelles driven by cytoplasmic dynein by calculating the ratio of minus-to-plus end reversions relative to the number of minus-end trajectories. A similar procedure was followed to calculate the reversion probability of melanosomes transported by kinesin-2. Table 1 shows that the reversion probability of each of the motors is similar during aggregation and dispersion suggesting that the reversion mechanism is independent from the stimulation condition of the cells.

On the other hand, the probability of switching motors for melanosomes initially driven by kinesin-2 is approximately twice the reversion probability of those driven by cytoplasmic dynein. In contrast to the increasing amount of information regarding the structure, regulation and biophysical properties of kinesin-1 and cytoplasmic dynein, little is known about the properties of kinesin-2 obscuring the interpretation of this result. Thus, the causes of this higher reversion probability of kinesin driven melanosomes remain to be determined.

A Model for Wave-Shaped Reversions

Figure 2 shows the distance traveled by a melanosome as a function of time during a representative reversion. The right panel of the figure shows that the speed of the melanosome before the reversion slowly decreases with time approaching zero then, the melanosome returns over the same path moving initially at a very high speed and slowing down with time. We found that 70% of the reversions present these wave-shaped distance versus time plots. The instantaneous speed during the first 30 ms after the reversal point (t_s in Fig. 2) was in average 1,900 ± 150 nm/s. This high speed cannot be explained by only considering the transport by microtubule-dependent molecular motors, which move at speeds in the range of 250–1,000 nm/s in melanophores of *Xenopus laevis* [11, 26].

Wave-shaped reversions present characteristics similar to those observed for trajectories of beads attached to motor molecules moving along microtubules in optical trapping experiments. The motor moves the beads far from the equilibrium position at the center of the trap while the trap applies an opposing force making the motor to slow down and stop when reaching stall force. It then detaches from the track and the bead moves fast to the equilibrium position at the trap center (see for example, [30, 31]).

Similarly, we propose that intracellular components in the overcrowded cytoplasm such as cytoskeletal filaments can act as obstacles which elastically interact with motor-

Journal : Large 12013 Dispatch : 28-10-2008 Pages : 11
Article No. : 9034 LE TYPESET
MS Code : EM522 CP DISK

Table 1 Statistics of melanosome transport

	Plus-end directed melanosomes (%)	Trajectories presenting reversions (%)	Wave shape-reversions (%)	Reversion probability for kinesin	Reversion probability for dynein
Dispersion	74	40	73	0.41	0.25
Aggregation	40	30	70	0.46	0.17

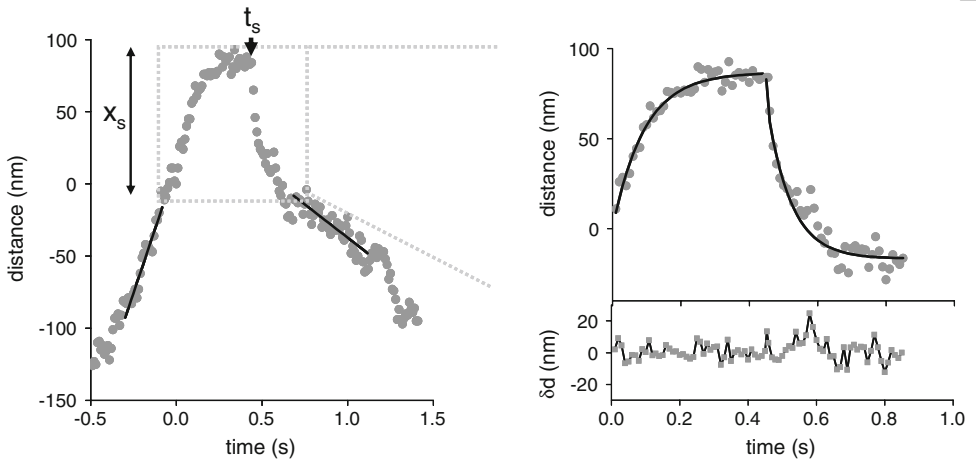

Fig. 2 Reversions characterization. Representative region of a trajectory showing a wave-shaped reversion. The distance traveled by the organelle was calculated as described in Materials and Methods and is represented as a function of time. The stall distance x_s and the reversion time t_s are marked with arrows. Continuous lines show the processive motion of the organelle before and after the interaction with the obstacle. Continuous lines in the right panel show the fitting of Eqs. 3 and 4 to the experimental data. The bottom panel shows the residuals obtained from the fitting

driven organelles. Melanosomes are in average 500 nm-diameter suggesting a high probability of encountering obstacles in the overcrowded cytoplasm.

The stochastic motion of the complex organelle-motor is governed by the Langevin equation [32, 33], which takes into account the Brownian force produced by collisions with other molecules as well as the viscous drag and other external forces. If the time scale of the Brownian force is much smaller than the time scale of other forces that might be involved in the motion of the motor-organelle complex, the temporal evolution of the position of the organelle can be described at long enough times in terms of a non-stochastic equation [34]. In this regime, the forces acting on the organelle are given by,

$$\mathrm{m}\frac{d^2x}{dt^2} = -\gamma\frac{dx}{dt} + F_{\mathrm{motor}} + F_{\mathrm{ext}} \qquad (1)$$

where x is the average distance traveled by the organelle, m is its mass, γ is a drag coefficient, F_{motor} is the force exerted by the motors driving the organelle and F_{ext} is an external force.

When the number of active motors and the viscous drag do not change during the transport, the speed of the organelle reaches a constant value v'_{d} in the absence of external forces. The system described by Eq. 1 will reach this stationary or Stokes regime [35] after a time t_{r} equal to m/γ [36]. This behavior is observed in experimental trajectories as periods of rectilinear motion of constant velocity, called "runs" [37].

Considering that the organelle moving at v'_{d} encounters an obstacle and that their interaction is elastic:

$$\mathrm{m}\frac{d^2x}{dt^2} + \gamma\frac{dx}{dt} + \kappa x = F_{\mathrm{motor}} \qquad (2)$$

where κ is the elastic constant characterizing the interaction.

Taking into account that the average melanosome diameter is 500 nm [24], its density is $\sim$1.2 g/ml [38] and $\gamma \sim 10^{-8}$ Ns/m for the drag coefficient in water [36], m/γ would be $\sim 10^{-2}$ μs, which is significantly lower than the temporal resolution of the tracking method we used. Since the viscosity of the cytosol is higher than that of aqueous solutions (see references in [39]), m/γ will be even lower than the value calculated above indicating that t_{r} is achieved instantaneously considering the time resolution of our experiments. In this condition, the dynamics of the system is reduced to an overdamped behavior.

The distance traveled by the organelle before the switch of direction is given by the solution of Eq. 2, which in the overdamped limit reduces to:

Journal : Large 12013 Dispatch : 28-10-2008 Pages : 11
Article No. : 9034 LE TYPESET
MS Code : EM522 CP DISK

$$x(t) = \frac{\gamma}{\kappa} v_d \left[1 - e^{-\frac{\kappa t}{\gamma}}\right] \quad 0 < t < t_s \tag{3}$$

Where $x(t = 0) = 0$. This equation shows that the moving melanosome slows down as a consequence of the opposing force introduced by the obstacle. This increasing, elastic force will also increase the probability of detachment of the active motors from the track [40, 41]. We postulate that at the reversal position x_s, the active motors detach from the microtubule and the melanosome starts moving in the opposite direction driven by opposed-polarity motors.

This proposition is based also on the facts that: (1) there are no evidences in the literature that microtubule-dependent motors responsible for melanosomes transport can move backward along microtubules and, (2) dynein and kinesin are not active simultaneously as was also mentioned in the "Introduction" section. The elastic energy released after the detachment of the first motors will also contribute to the backward motion of the melanosome.

By following an analysis similar to that described before, it can be demonstrated that the distance traveled by the organelle after the switch of direction is given by:

$$x(t) = \left[x_s + \frac{\gamma}{\kappa} v'_d\right] e^{\frac{\kappa}{\gamma}(t_s - t)} - v'_d \frac{\gamma}{\kappa} \quad t_s < t \tag{4}$$

where t_s is the switch time, $x(t = t_s) = x_s$ and v'_d is the speed of the motors that drive the organelle after the reversion.

Equations 3 and 4 consider that if several motors are driving the organelle, they would act in concert transporting the cargo together until detaching from the track or after attaching back to it. Welte et al. [14] measured in vivo the stall force of lipid droplets transported in *Drosophila* embryos during different stages of development. They determined that the stall force changes among these stages in a quantized fashion, consistent with a variation in the number of active motors driving the droplets. They did not observe at any of these development stages a distribution of stall forces compatible with motors detaching one-by-one. This result is different from what it would be expected according to a model describing in vitro transport of cargos driven by multiple copies of motors under load [42]. The reason that might explain this divergence is that, as it is indicated by Welte et al. [14], specific proteins would enforce the coordination of same polarity motors in vivo and control the number of actively engaged motors.

Trajectories Analysis

Wave Shape-Reversions Are Characteristic of Fast-Moving Organelles

We fit Eqs. 3 and 4 to the segments obtained before and after the reversal position, respectively, considering the same set of γ and κ for each analyzed reversion. These parameters characterize the interaction of the organelle with the obstacle and the medium and, in a first approximation, can be considered to be the same before and after the encounter.

The fitting of the equations was done by minimizing the function: $S = \sum_i (X(t_i) - x_i)^2$, where $X(t_i)$ is the prediction of the model for the position of the melanosome at time t_i, and x_i is the corresponding experimental data. Fitting routines were written within the MatLab programing environment (The MathWorks, Natick, MA), using the genetic algorithm toolbox.

Figure 3a shows the distribution of v'_d obtained by fitting Eqs. 3 and 4 to wave-shaped reversions during aggregation and dispersion. We then classified v'_d values according to the motor that was driving the organelle before the reversion and found that the distribution of this parameter was not significantly different for kinesin- and dynein-driven melanosomes (>0.77 confidence level, Kolmogorv–Smirnov test [43]).

The histogram of v'_d—which is obtained by only analyzing regions of the trajectories presenting reversions—can be compared to the speed distribution we have previously obtained by analyzing the complete trajectories of melanosomes driven by dynein and kinesin [26]. Briefly, in that previous work we found that melanosomes speed followed a multi-peak distribution that could be explained considering that this parameter depends linearly on the number of active motors. We also found that melanosomes transported by a single dynein or kinesin molecule were the predominant population during aggregation and dispersion and that their speed was $\sim$250 nm/s.

We cannot discard the presence of multiple peaks in the v'_d distribution; however, we do not have enough information to statistically analyze this possibility since reversals represent only a small region of the trajectories.

On the other hand, Fig. 3a shows that the v'_d distribution presents a maximum at $\sim$0.5 μm/s indicating that wave-shaped reversions are detected only in those regions of the trajectories in which melanosomes are moving fast and are probably transported by more than 1 copy of the active motor.

The Switch Occurs Once the Motor Reaches Stall Condition

Equations 3 and 4 show a strong dependence with γ/κ ratio but not with the independent parameters and thus, they cannot be recovered individually from the fitting. γ/κ represents the time constant of the elastic response, i.e., low values of γ/κ imply that the obstacle stiffness is high and thus the organelle stops shortly after their interaction. This

Journal : Large 12013 | Dispatch : 28-10-2008 | Pages : 11
Article No. : 9034 | LE | TYPESET
MS Code : EM522 | CP | DISK

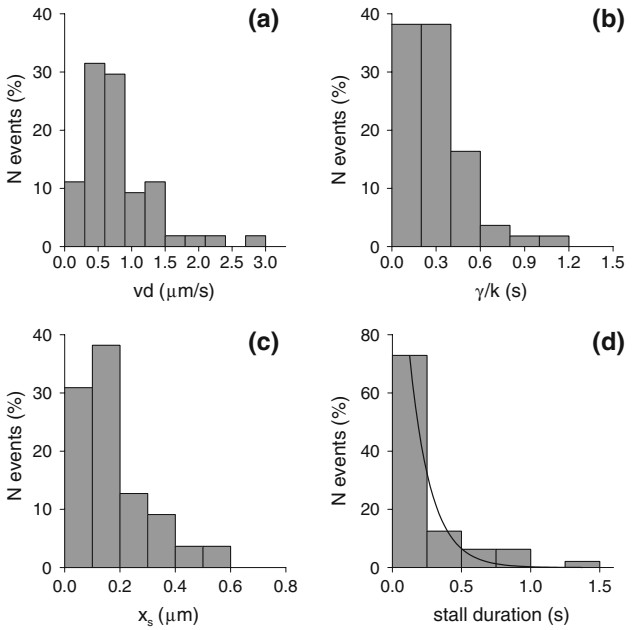

Fig. 3 Distribution of parameters characterizing reversions in melanosomes transport direction. **a** Distribution of melanosomes speed before interacting with the obstacle. **b** Distribution of characteristic times of the interaction with the obstacle. The mean γ/κ value is 290 ± 30 ms. v'_d and γ/κ values were obtained by fitting Eqs. 3 and 4 to wave-shaped reversions in melanosomes trajectories. **c** Distribution of stall distances calculated by using Eq. 5. The average stall distance was 200 ± 30 nm. **d** Distribution of stall duration. Stall duration is defined as the interval of time the organelle spends in stall conditions before it reverts its direction of motion. The continuous line corresponds to the fitting of an exponential-decay function, with a characteristic time constant of 160 ± 2 ms. Characteristic parameters of the distributions are expressed as the mean ± standard error. Histograms were constructed setting the bin size to the value determined by the commonly used criterion [53]:bin size $= 3.49\frac{s}{n^{1/3}}$ where n is the number of data and s is an estimate of the standard deviation

parameter shows a wide distribution with a mean value of 290 ± 30 ms (Fig. 3b). The average γ/κ value obtained in this work is in the order of the values expected according to the typical elasticities of intracellular elements [36, 44, 45] and of γ values determined in the cytoplasm [39]. This result confirms that the response time of the elastic interaction is higher than the time resolution of the tracking method allowing the direct observation of the time evolution of the system.

This result is not compatible with a model in which reversions are initiated by a sudden stop of the active motor. If this was the case, wave-shaped distance versus time plots would be the consequence of the motion of the melanosome caused by inertia once the motor stops moving. The time constant of the inertial effects is lower than 10^{-2} μs as we discussed previously. If we also consider the stiffness of the motor to stretching κ_e [45, 46] the time constant would be $\gamma/\kappa_e \sim 0.03$ s. These values are significantly lower than that measured in this work (Fig. 3b) and thus this hypothesis can be ruled out.

According to Eq. 2, we can define the stalling distance x_s as the theoretical distance traveled by the melanosome from the moment it contacts the spring-like obstacle until its maximal compression:

$$x_s = \frac{\gamma}{\kappa} v_d \tag{5}$$

Figure 3c shows the distribution of stalling distance determined by using this equation. The average value was 200 ± 30 nm.

We can also estimate the distance traveled by the melanosome since it starts interacting with the elastic obstacle until it switches the direction, i.e., the switch distance. The algorithm described in "Materials and Methods" section can easily recognize the reversion position and the initial point of the interaction can be detected by the sudden decrease of the organelle speed.

We calculated the ratio between the stall and switch distances and observed that this ratio is not significantly different from 1 (Student's t test, 95% confidence). This result suggests that reversions can only occur once the motors responsible for the motion reach stall conditions.

The Detachment of the Organelle Is Stochastic

To further characterize the mechanism that triggers the exchange of motors we measured the stall duration, i.e., the period that the organelle spends in stall conditions before it reverts its direction. Since the start of a plateau was not always sharply defined because some curves approached it asymptotically, we arbitrarily determined the stall duration from the moment the organelle travel at speeds lower than 50 nm/s to the switch time t_s.

Figure 3d shows that the stall duration distribution follows an exponential-decay function with a characteristic time of 0.16 ± 0.02 s. This behavior indicates that the detachment probability during stall is constant as would be expected according to the stochastic nature of the switch.

This result agrees with those obtained in optical trapping experiments of kinesin-attached beads moving along microtubules: Coppin et al. [41] also observed an exponential-decay distribution for the stall duration measured when the beads are far from the trap center. Interestingly, these authors also verified that the dissociation rate of the motors from the track is independent of load once the motor stalls.

Our model is consistent with the observation of the independence of the reversion probability with the stimulation state of melanophores (Table 1) since reversions only depend on the probability of encountering an obstacle. This probability would not depend on the stimulation state of melanophores since the viscoelastic properties of the

Journal : Large 12013 Dispatch : 28-10-2008 Pages : 11
Article No. : 9034 LE TYPESET
MS Code : EM522 CP DISK

cytoplasm of *Xenopus laevis* melanophores are not significantly different during aggregation and dispersion as suggested by preliminary results from our group using single particle tracking microrheology (for a description of this technique see [47, 48]).

The Second Motor Attaches to the Track After Complete Relaxation of the Elastic Interaction

In half of the analyzed wave-shaped reversions, the second motor attaches to the track once the melanosome stops moving (i.e., $v'_d = 0$ μm/s). Visual examination of these reversions shows that after elastic relaxation, melanosomes generally stay still for a short period of time (<0.2 s) and, immediately after that, almost all melanosomes start moving in the opposite direction in a stationary fashion (95%). The mean speed of this processive motion was 300 ± 30 nm/s, which is compatible with a melanosome moving with a single motor copy.

Since the fast, backward motion usually takes ∼300 ms to complete and occurs near the microtubule along which the melanosome was originally moving, there is a high probability that this microtubule is very close to the organelle and thus active transport will resume on the same microtubule. However, in some cases melanosomes could reattach to a different microtubule. If the second microtubule is located close to the initial microtubule, the reversion will be detected by the reversal finding algorithm. Otherwise this motion will be observed not as a reversion but as a change of direction. Therefore, we are probably underestimating the frequency of events involving switches of microtubule motors.

On the other hand, in the last year it has been demonstrated that myosin-V diffuses along microtubules [49] and enhances significantly the processive run length of kinesin-1 when both motors are present on the same cargo. These authors proposed that myosin-V can act as a tether preventing kinesin from diffusing away from the track. In the particular case of melanophores, it might be possible that myosin-V could also tether melanosomes to microtubule; however, there are not experimental evidences to support this hypothesis.

30% of the data shows v'_d values with a similar distribution of that observed for v'_d (not shown). The rest of the data could not be classified because they did not show a satisfactory fitting after the reversion point. This could be probably consequence of other processes affecting the trajectories of the organelles (e.g., a collision with a second obstacle).

Peak-Shaped Reversions

In this work, we have analyzed wave-shaped reversions which, as we mentioned before, are characteristic of fast-moving organelles. We also detected some reversions (24%) which show distinct properties with respect to wave-shaped reversions (Fig. 4). In these peak reversions, the speed was approximately constant before and after the switch time. Interestingly, these reversions were observed

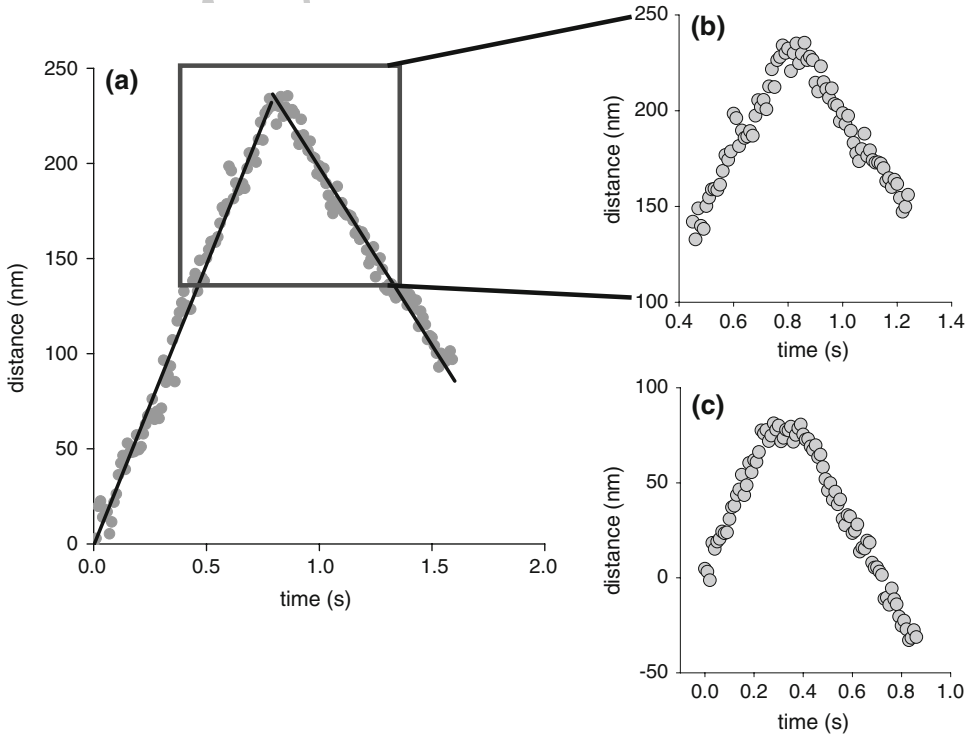

Fig. 4 Peak-shaped reversions. **a** Distance traveled by a melanosome as a function of time for a representative peak-shaped reversion. The speeds of the organelle before and after the switch were 300 nm/s and 200 nm/s, respectively. **b** Zoom of the reversion showed in (**a**) near the switch point. The stall duration is ∼0.1 s. **c** Simulated peak-shape reversion. The trajectory was obtained using Eqs. 3 and 4 with parameters values $v'_d = 320$ nm/s, $\gamma/\kappa = 0.03$ s, $v'_d = -250$ nm/s and stall duration equal to 160 ms, which corresponds to the characteristic stall duration determined in Fig. 3d. Random noise with the same distribution and amplitude of the experimental one was added to the simulated data to make the comparison easier

Journal : Large 12013 Dispatch : 28-10-2008 Pages : 11
Article No. : 9034 LE TYPESET
MS Code : EM522 CP DISK

for organelles moving at average speeds of 320 ± 40 nm/s, compatible with transport with a single motor copy [26].

These distinct characteristics may suggest that a different switching mechanism is responsible for peak reversions. However, Eq. 5 shows that the stall distance decreases with both v_d and γ/κ. We observed that by using a set of v_d and γ/κ values slightly lower than the mean parameters obtained from wave-shaped reversions we do recover plots with similar properties of those corresponding to experimental peak-shaped reversions. For example, the simulated reversion showed in Fig. 4c resulted from using a γ/κ value that is 10% lower than the mean value determined from Fig. 3b. Importantly, the v_d and γ/κ set of values that resulted in the peak-shaped reversion shown in this example are within the range of the experimental values determined for waved-shaped reversions (Fig. 3a and b).

We would have expected a higher proportion of peak-shape reversions since most of the time melanosomes are transported at ∼250 nm/s [26]. However, these organelles are expected to show shorter stall distances as we demonstrated above and shorter run lengths as it is observed during the transport of lipid droplets [37]. Thus, these reversions are probably not detected by the reversion-finder algorithm.

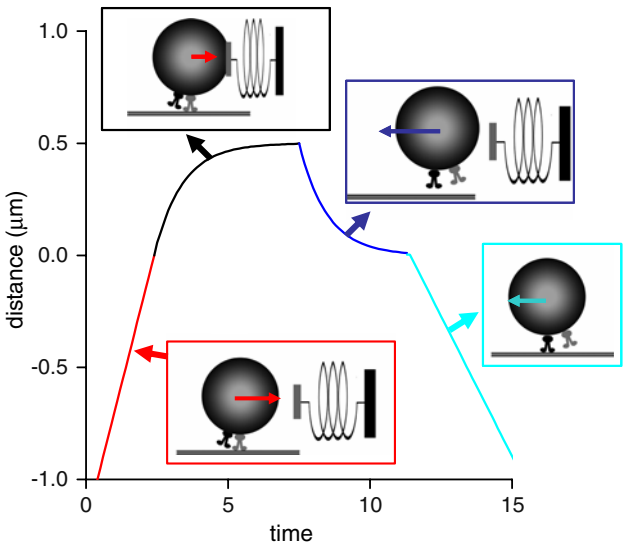

Fig. 5 Scheme of the switch mechanism triggered by an elastic interaction between a motor-driven melanosome and an obstacle. The organelle travels along the microtubule at a constant speed (red) until it approaches to the obstacle and start interacting with it (black). As a consequence, the melanosome slows down. Once the opposing force equals the stall force of the motor, it detaches from the track and start moving against the viscous drag (blue). After relaxation of the system, the opposite polarity motor attaches to the track and continues moving in opposite direction (cyan). The scheme considers the case in which $v'_d = 0$. To simplify the scheme, a single copy of each family of motors is represented

Concluding Remarks

In this work, we have studied the characteristics of trajectories of melanosomes moving along microtubules and focused on those regions showing reversions in the direction of transport to get insight into the mechanism that triggers the switch between microtubule motors of opposed polarity.

Most of the studied reversions could be explained according to the model schematically represented in Fig. 5. According to our results, an obstacle in the cytosol introduces an extra load to the active motors that make them slow down and stop when the force generated by the motor molecules equals the opposite force, i.e., the drag force plus the force exerted by the spring-like obstacle. Once this stall condition is reached, the active motor stochastically detaches from the microtubule track. In this condition, the free organelle moves backwards at high initial speeds and slows down as a consequence of the friction with the medium. Once the organelle stops moving and, since it is near the track, opposite polarity motors can attach to the microtubule and transport the organelle in the opposite direction.

Our model considers that the melanosome behaves as a stiff bead. In a recent article, Guo et al. [50] measured the Young modulus of melanosomes and found that they are considerably higher than the modulus of organelles with cytoplasm (<1 MPa) and approaching values of the modulus of protein crystals (∼100 MPa). Despite these measurements were done on melanosomes of human retinal pigment epithelium, their properties are not expected to be very different from those of *Xenopus laevis* melanophores and thus the latter can be considered as stiff organelles.

The postulated model gives an explanation to the trigger of the switch of motors, but does not explain how the coordination of the motors is achieved. We can hypothesize that the collision determines the end of a run of a given polarity motor and the regulatory proteins (e.g., dynactin) involved in the coordination mechanism would define which motor will be turned on after this collision and keep motors of opposite polarity in the inactive state.

The model postulated in this work agrees with previous results from Gross et al. [37] who postulated that there is a mechanism that ends runs of dynein-driven organelles before the motors fall off the microtubules which acts with a constant probability per unit distance, and is typically coupled to a switch in travel direction. They also proposed that a similar mechanism governs plus-end motion, and its regulation controls the net direction of transport.

Also, the model gives a possible explanation to previous results from Rogers et al. [24] who observed that melanosomes transport in vitro process over longer distances that in vivo. The main difference between both assays is the environment in which the transport occurs: while in

Journal : Large 12013 Dispatch : 28-10-2008 Pages : 11
Article No. : 9034 LE TYPESET
MS Code : EM522 CP DISK

vitro assays are done in aqueous solutions, the cytoplasm is a crowded, viscoelastic medium and the probability of finding obstacles that decreases the run length and increases the probability of switching motors is higher.

As it is explained by Gross [1], the frequent changes of directions observed for several cargoes in the cell cytoplasm seems to be an inefficient mechanism to move the cargoes to a given, particular location. In the same way, transport toward a particular region of the cell will be delayed if the encounters with obstacles trigger the switch of microtubule-dependent motors. However, in the absence of a reversion mechanism, motor-driven organelles would remain in a fixed position after encountering an obstacle until the obstacle or the complex moves away. Since the cytoplasm is an overcrowded medium with a high concentration of obstacles, the efficiency and regulation of the transport will be highly impaired in this situation.

On the other hand, if the encounter with the obstacle triggers the exchange of motors, the cargoes would back up and move in the opposite direction. Eventually, it may switch to a different microtubule that crossed the path and find an alternative route to evade the obstacle. This mechanism would contribute to avoid "traffic jams" such as those observed in axons, which have been proposed as the crucial injury in a range of neurodegenerative diseases [51, 52].

This research was supported by the ANPCyT (Argentina, PICT 31975) L.B, M.M.E and V.L. are members of the Carrera del Investigador Científico (CONICET). We acknowledge useful conversations with D. R. Parisi and P. Balenzuela.

Supporting File

Movie 1. Typical tracking experiment showing a reversion in a melanosome trajectory. The movie shows a $24 \times 24\ \mu m^2$ region of the cell (in pseudo color); melanosomes are observed in yellow. The black line shows the trajectory recover by the pattern-recognition algorithm. The total duration of the tracking experiment is 20 s.

References

1. Gross, S. P. (2004). Hither and yon: A review of bi-directional microtubule-based transport. *Physical Biology, 1*, R1–R11.
2. Suomalainen, M., Nakano, M. Y., Keller, S., Boucke, K., Stidwill, R. P., & Greber, U. F. (1999). Microtubule-dependent plus- and minus end-directed motilities are competing processes for nuclear targeting of adenovirus. *Journal of Cell Biology, 144*, 657–672.
3. Smith, G. A., Gross, S. P., & Enquist, L. W. (2001). Herpesviruses use bidirectional fast-axonal transport to spread in sensory neurons. *Proceedings of the National Academy of Sciences of the United States of America, 98*, 3466–3470.
4. Shah, J. V., Flanagan, L. A., Janmey, P. A., & Leterrier, J. F. (2000). Bidirectional translocation of neurofilaments along microtubules mediated in part by dynein/dynactin. *Molecular Biology of the Cell, 11*, 3495–3508.
5. Hollenbeck, P. J. (1996). The pattern and mechanism of mitochondrial transport in axons. *Frontiers in Bioscience, 1*, d91–d102.
6. Hollenbeck, P. J. (1993). Products of endocytosis and autophagy are retrieved from axons by regulated retrograde organelle transport. *Journal of Cell Biology, 121*, 305–315.
7. McDonald, D., Vodicka, M. A., Lucero, G., Svitkina, T. M., Borisy, G. G., Emerman, M., et al. (2002). Visualization of the intracellular behavior of HIV in living cells. *Journal of Cell Biology, 159*, 441–452.
8. Valetti, C., Wetzel, D. M., Schrader, M., Hasbani, M. J., Gill, S. R., Kreis, T. E., et al. (1999). Role of dynactin in endocytic traffic: Effects of dynamitin overexpression and colocalization with CLIP-170. *Molecular Biology of the Cell, 10*, 4107–4120.
9. Welte, M. A. (2004). Bidirectional transport along microtubules. *Current Biology, 14*, R525–R537.
10. Gross, S. P., Welte, M. A., Block, S. M., & Wieschaus, E. F. (2002). Coordination of opposite-polarity microtubule motors. *Journal of Cell Biology, 156*, 715–724.
11. Gross, S. P., Tuma, M. C., Deacon, S. W., Serpinskaya, A. S., Reilein, A. R., & Gelfand, V. I. (2002). Interactions and regulation of molecular motors in *Xenopus* melanophores. *Journal of Cell Biology, 156*, 855–865.
12. Schroer, T. A. (2004). Dynactin. *Annual Review of Cell and Developmental Biology, 20*, 759–779.
13. Gross, S. P. (2003). Dynactin: Coordinating motors with opposite inclinations. *Current Biology, 13*, R320–R322.
14. Welte, M. A., Gross, S. P., Postner, M., Block, S. M., & Wieschaus, E. F. (1998). Developmental regulation of vesicle transport in *Drosophila* embryos: Forces and kinetics. *Cell, 92*, 547–557.
15. Deacon, S. W., Serpinskaya, A. S., Vaughan, P. S., Lopez Fanarraga, M., Vernos, I., Vaughan, K. T., et al. (2003). Dynactin is required for bidirectional organelle transport. *Journal of Cell Biology, 160*, 297–301.
16. Berezuk, M. A., & Schroer, T. A. (2007). Dynactin enhances the processivity of kinesin-2. *Traffic, 8*, 124–129.
17. King, S. J., & Schroer, T. A. (2000). Dynactin increases the processivity of the cytoplasmic dynein motor. *Nature Cell Biology, 2*, 20–24.
18. Nascimento, A. A., Roland, J. T., & Gelfand, V. I. (2003). Pigment cells: A model for the study of organelle transport. *Annual Review of Cell and Developmental Biology, 19*, 469–491.
19. Rozdzial, M. M., & Haimo, L. T. (1986). Bidirectional pigment granule movements of melanophores are regulated by protein phosphorylation and dephosphorylation. *Cell, 47*, 1061–1070.
20. Sammak, P. J., Adams, S. R., Harootunian, A. T., Schliwa, M., & Tsien, R. Y. (1992). Intracellular cyclic AMP not calcium, determines the direction of vesicle movement in melanophores: Direct measurement by fluorescence ratio imaging. *Journal of Cell Biology, 117*, 57–72.
21. Tuma, M. C., Zill, A., Le Bot, N., Vernos, I., & Gelfand, V. (1998). Heterotrimeric kinesin II is the microtubule motor protein responsible for pigment dispersion in *Xenopus* melanophores. *Journal of Cell Biology, 143*, 1547–1558.

22. Nilsson, H., & Wallin, M. (1997). Evidence for several roles of dynein in pigment transport in melanophores. *Cell Motility and the Cytoskeleton, 38*, 397–409.
23. Rogers, S. L., & Gelfand, V. I. (1998). Myosin cooperates with microtubule motors during organelle transport in melanophores. *Current Biology, 8*, 161–164.
24. Rogers, S. L., Tint, I. S., Fanapour, P. C., & Gelfand, V. I. (1997). Regulated bidirectional motility of melanophore pigment granules along microtubules in vitro. *Proceedings of the National Academy of Sciences of the United States of America, 94*, 3720–3725.
25. Thompson, R. E., Larson, D. R., & Webb, W. W. (2002). Precise nanometer localization analysis for individual fluorescent probes. *Biophysical Journal, 82*, 2775–2783.
26. Levi, V., Serpinskaya, A. S., Gratton, E., & Gelfand, V. (2006). Organelle transport along microtubules in *Xenopus* melanophores: Evidence for cooperation between multiple motors. *Biophysical Journal, 90*, 318–327.
27. Gelles, J., Schnapp, B. J., & Sheetz, M. P. (1988). Tracking kinesin-driven movements with nanometre-scale precision. *Nature, 331*, 450–453.
28. Yildiz, A., Tomishige, M., Vale, R. D., & Selvin, P. R. (2004). Kinesin walks hand-over-hand. *Science, 303*, 676–678.
29. Levi, V., Gelfand, V. I., Serpinskaya, A. S., & Gratton, E. (2006). Melanosomes transported by myosin-V in *Xenopus* melanophores perform slow 35 nm steps. *Biophysical Journal, 90*, L7–L9.
30. Svoboda, K., & Block, S. M. (1994). Force and velocity measured for single kinesin molecules. *Cell, 77*, 773–784.
31. Carter, N. J., & Cross, R. A. (2005). Mechanics of the kinesin step. *Nature, 435*, 308–312.
32. Wang, H. (2006). Motor potential profile and a robust method for extracting it from time series of motor positions. *Journal of Theoretical Biology, 242*, 908–921.
33. Lukić, B., Jeney, S., Sviben, Ž., Kulik, A. J., Florin, E., & Forró, L. (2007). Motion of a colloidal particle in an optical trap. *Physical Review E, 76*, 011112.
34. Reichl, L. E. (1988). *A modern course in statistical physics*. Austin, Texas: University of Texas press.
35. Lifshitz, E. M., & Landau, L. D. (1987). *Fluid mechanics*. Oxford: Butterworth-Heinemann.
36. Howard, J. (2001). *Mechanics of motor proteins and the cytoskeleton*. Sunderland, MA: Sinauer Associates.
37. Gross, S. P., Welte, M. A., Block, S. M., & Wieschaus, E. F. (2000). Dynein-mediated cargo transport in vivo. A switch controls travel distance. *Journal of Cell Biology, 148*, 945–956.
38. Sharma, S., Wagh, S., & Govindarajan, R. (2002). Melanosomal proteins-role in melanin polymerization. *Pigment Cell Research, 15*, 127–133.
39. Yamada, S., Wirtz, D., & Kuo, S. C. (2000). Mechanics of living cells measured by laser tracking microrheology. *Biophysical Journal, 78*, 1736–1747.
40. Leduc, C., Ruhnow, F., Howard, J., & Diez, S. (2007). Detection of fractional steps in cargo movement by the collective operation of kinesin-1 motors. *Proceedings of the National Academy of Sciences of the United States of America, 104*, 10847–10852.
41. Coppin, C. M., Pierce, D. W., Hsu, L., & Vale, R. D. (1997). The load dependence of kinesin's mechanical cycle. *Proceedings of the National Academy of Sciences of the United States of America, 94*, 8539–8544.
42. Klumpp, S., & Lipowsky, R. (2005). Cooperative cargo transport by several molecular motors. *Proceedings of the National Academy of Sciences of the United States of America, 102*, 17284–17289.
43. Conover, W. J. (1999). *Practical nonparametric statistics*. New York: Wiley.
44. Gardel, M. L., Shin, J. H., MacKintosh, F. C., Mahadevan, L., Matsudaira, P., & Weitz, D. A. (2004). Elastic behavior of cross-linked and bundled actin networks. *Science, 304*, 1301–1305.
45. Kawaguchi, K., Uemura, S., & Ishiwata, S. (2003). Equilibrium and transition between single- and double-headed binding of kinesin as revealed by single-molecule mechanics. *Biophysical Journal, 84*, 1103–1113.
46. Jeney, S., Stelzer, E. H., Grubmuller, H., & Florin, E. L. (2004). Mechanical properties of single motor molecules studied by three-dimensional thermal force probing in optical tweezers. *Chemphyschem, 5*, 1150–1158.
47. Mason, T. G., Ganesan, K., van Zanten, J. H., Wirtz, D., & Kuo, S. C. (1997). Particle tracking microrheology of complex fluids. *Physical Review Letters, 79*, 3282–3285.
48. Tseng, Y., Kole, T. P., & Wirtz, D. (2002). Micromechanical mapping of live cells by multiple-particle-tracking microrheology. *Biophysical Journal, 83*, 3162–3176.
49. Ali, M. Y., Krementsova, E. B., Kennedy, G. G., Mahaffy, R., Pollard, T. D., Trybus, K. M., et al. (2007). Myosin Va maneuvers through actin intersections and diffuses along microtubules. *Proceedings of the National Academy of Sciences of the United States of America, 104*, 4332–4336.
50. Guo, S., Hong, L., Akhremitchev, B. B., & Simon, J. D. (2008). Surface elastic properties of human retinal pigment epithelium melanosomes. *Photochemistry and Photobiology, 84*, 671–678.
51. Goldstein, L. S. (2001). Kinesin molecular motors: Transport pathways, receptors, and human disease. *Proceedings of the National Academy of Sciences of the United States of America, 98*, 6999–7003.
52. Hurd, D. D., & Saxton, W. M. (1996). Kinesin mutations cause motor neuron disease phenotypes by disrupting fast axonal transport in *Drosophila*. *Genetics, 144*, 1075–1085.
53. Scott, D. W. (1979). On optimal and data-based histograms. *Biometrika, 3*, 605–610.

Humana Press

Journal : **Large 12013** Dispatch : **28-10-2008** Pages : **11**
Article No. : **9034** ☐ LE ☐ TYPESET
MS Code : **EM522** ☑ CP ☑ DISK